

Design of Optical Components for a Light Emitting Diode Zoom Illumination System

Yen-Pin TSAI and Chinghua HUNG*

Department of Mechanical Engineering, National Chiao Tung University,
1001 Ta Hsueh Road, Hsinchu 300, Taiwan, R.O.C.

(Received July 21, 2010; Accepted January 19, 2011)

In this article, we report an optical design for a light emitting diode that can achieve high illumination quality using two hyperbolic reflectors. The relative movements of the reflectors and the light source produce a zoom function that can change the illumination beam from convergence to divergence. This study uses optical software ZEMAX for system simulation, and optimization was performed to select reflector parameters with the objectives of both improving floodlight uniformity and spotlight efficiency. Finally, experiments were conducted to verify the validity of the design, and the results corresponded well to the zoom illumination simulations.

© 2011 The Japan Society of Applied Physics

Keywords: hyperbolic, reflector, LED, illumination, optimization

1. Introduction

Light emitting diode (LED) has the characteristics of high efficiency, low power consumption, low driving voltage, low heat generation, and longevity. In addition, they contain no mercury, and thus create fewer problems during recycling. For these reasons, the use of LEDs is a good solution for environmental protection.¹⁾

Current applications of LEDs in illumination include (i) LEDs arranged as an array that radiates light directly; (ii) LEDs placed inside reflectors, with rays reflected to the target by the reflectors; and (iii) LEDs placed behind lenses, with refraction or total internal reflection guiding rays to the target. Using these methods, LED light can be effectively collected or radiated to particular positions.

Since the shape of optical elements is difficult to modify during usage, the rays are fixed and there is generally only one use for one design. However, different situations call for different lighting requirements. In some cases, a focused spotlight is needed to send light far away, while floodlighting is necessary to spread light to illuminate a large area. Illumination systems with a zoom function can adjust the area of illumination depending on user requirements using just one apparatus. Hence, zoom illumination designs are worth studying for their potential savings in space and cost.

Reflectors can catch and redirect the radiant flux of a light source. By carefully designing the shape and size of the specular surfaces, useful beams of light can be created.²⁾ Recently, aspheric reflectors have been widely applied in optical designs. Tsuei *et al.*³⁾ used three kinds of reflector, a 45 bevel reflector, a parabolic reflector, and an ellipsoidal reflector, in indoor LED lighting design, and the result showed the potential advantages of LED lighting in the future. Hwang *et al.*⁴⁾ successfully performed numerical and experimental analyses on an aspheric reflector mirror for an infrared surveillance camera.

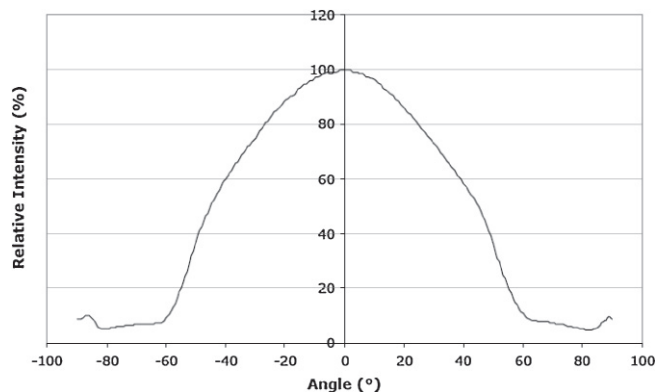


Fig. 1. Spatial distributions of luminous intensity for Cree Xlamp XR-E P4 LEDs.²⁾

LEDs emit light as a surface source rather than an ideal point source, and the spatial distributions of their luminous intensity are not uniform because of a cover lens. Figure 1 shows the spatial distribution of luminous intensity of the Cree Xlamp XR-E P4 LEDs⁵⁾ used in this research. It is difficult to calculate the detailed behavior of LED lights. However, the recent development of more powerful computers has dramatically improved the ability to design and optimize complex systems.⁶⁾ Therefore, this study uses computer simulations to not only predict precise illumination patterns, but also to optimize the parameters of the proposed LED zoom illumination design.

2. Concept

This study presents a novel design using hyperbolic reflectors to achieve the objective of zoom illumination. The optical system is axially symmetric, and the LED emitting direction is set to the right. Figure 2(a) traces the rays of a moving LED light source with a single hyperbolic reflector. The proposed design simplifies the LED light source as a

*E-mail address: chhung@mail.nctu.edu.tw

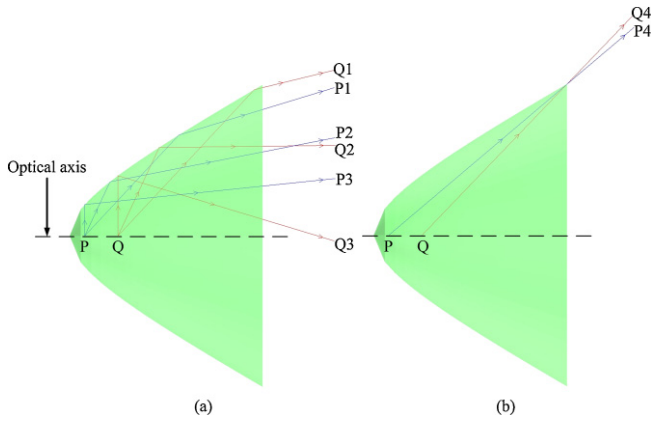


Fig. 2. (Color online) Ray tracing of a moving light source with a single hyperbolic reflector for (a) rays reflected by the reflector and (b) rays just missing the outer edge of the reflector.

point source with the characteristic of spatial distribution of luminous intensity, as Fig. 1 indicates. When the source is at position P, the three resulting rays are defined as P1, P2, and P3 based on their different angles to the optical axis. The corresponding rays when the source moves forward to position Q are Q1, Q2, and Q3. Rays Q1 and Q2 radiate out of the reflector at smaller angles to the optical axis than P1 and P2 do, respectively. Hence, the rays converge forward as the source moves from position P to Q. Although Q3 shows dispersion when the source moves forward, the energy of the large angle emitting ray of an LED light would be low due to the spatial distribution of luminous intensity. This means that the effect of dispersion on the final illumination is not noticeable. Focusing illumination is gradually formed as the LED light source moves forward, effectively achieving the function of zoom illumination.

As the source moves forward, the number of rays not controlled by the reflector, but radiating directly, increases. Figure 2(b) shows that rays P4 and Q4 just miss the outer edge of the reflector. The angle between ray Q4 and the optical axis is greater than that between ray P4 and the optical axis, increasing the directly radiating rays. Hence, the area of illumination is enlarged. However, it conflicts with the pre-assumption that the light will be focused by moving the source forward. To modify this condition, an outer reflector is added to the original reflector system, as Fig. 3(a) indicates. The outer reflector then reflects the rays between P4 and P5 and converges these rays forward. Figure 3(b) shows that the more the rays radiate directly during the focusing process, the farther forward the outer reflector must move to simultaneously intercept the additional rays. The interaction between the outer reflector and the source is identical to that between the inner reflector and the source, so the outer reflector must also have a hyperbolic shape.

3. Optical Simulation

This study includes optical simulations to assist the design with the consideration of the real emitting characteristics of

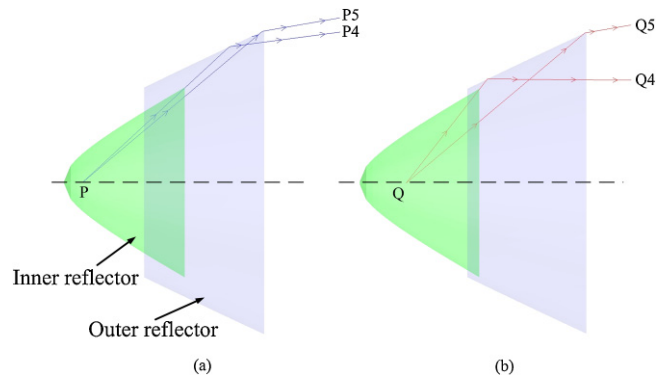


Fig. 3. (Color online) Ray tracing on the outer reflector (a) before the source moves forward and (b) after both the source and the outer reflector move forward.

Table 1. Initial reflector parameters.

Reflector	c^{-1} (mm)	k	Max. aperture (mm)	Min. aperture (mm)
Inner	0.1	-1.3	9	3.5
Outer	2	-1.1	15	9.25

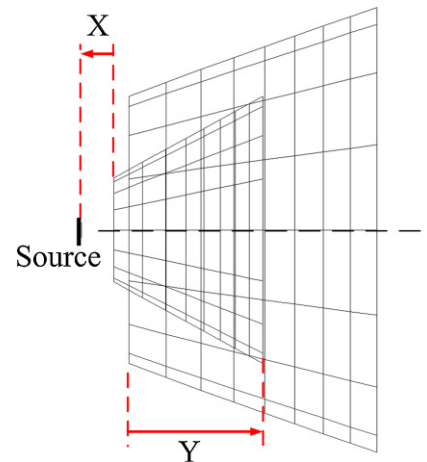


Fig. 4. (Color online) Relations of components.

an LED light source. ZEMAX⁷⁾ was used as the simulation tool in this research.

3.1 Model and light source

Reflective surface models were built for the simulation in the research. The standard aspheric function was used as follows:

$$z = \frac{cr^2}{1 + \sqrt{1 - (1+k)c^2r^2}} + \alpha_1r^4 + \alpha_2r^6 + \alpha_3r^8 + \dots, \quad (1)$$

where c is the base curvature at the vertex, and k is a conic constant.²⁾ Table 1 lists the initial parameters of the reflectors. Both reflectors are assumed to be perfect mirrors.

Figure 4 shows the definition of the relative position of the components. The X-value (positive toward the left)

Table 2. Initial zoom process settings.

	Configuration		
	A	B	C
X (mm)	2	0	-2
Y (mm)	9	5	1

indicates axial displacement measured from the position of the minimum aperture of the inner reflector to the light source, and the *Y*-value (positive toward the right) indicates axial displacement measured from the position of the minimum aperture of the outer reflector to the position of the maximum aperture of the inner reflector. Table 2 shows the initial displacement settings for three configurations within the considered zoom range. Configuration A provides the broadest floodlight, configuration C creates the most concentrated spotlight, and configuration B is the middle setting between the two conditions above.

CREE XLamp XR-E P4 LEDs have been used in many new designs, and were also used in this research. The flux performance of this type of LED is 80 lm, with an operation current of 350 mA and emitting area of $1 \times 1 \text{ mm}^2$. Figure 1 shows the spatial distribution of luminous intensity, which was used in this study to model the light source.

A $1 \times 1 \text{ m}^2$ detector was placed at a distance of 1 meter in front of the LED light source to serve as the target zone.

3.2 Ray tracing and results

Ray tracing was executed with 5,000,000 rays. To prove the concept that a single hyperbolic reflector can form zoom illumination, simulations were firstly performed with a single inner reflector. Figure 5(a) shows the illuminance maps with the same contour scales. During the zoom process from configuration A to C, the floodlight range decreases in diameter from about 80 to 40 cm. At the same time, the illuminance of the central spotlight was enhanced, and the maximum illuminance increased from 122 to 289 lx, thus confirming the effect of zoom illumination. Figure 5(b) shows the illuminance maps of three configurations with both inner and outer reflectors. During the zoom process, the floodlight range is the same as that in Fig. 5(a), while the maximum illuminance of the central spotlight increased from 124 to 2478 lx.

Figure 6 shows the cross-sectional illuminance values. The total illuminance is the sum of the three types of ray, including the inner reflector reflected rays, the outer reflector reflected rays, and directly radiating rays. The illuminance distribution caused by the inner reflector is consistent with the floodlight pattern, while rays reflected by the outer reflector dominate the high illuminance of the spotlight, and have no effect on the floodlight. Consequently, the inner reflector governs the floodlight and the outer reflector dominates the spotlight.

This study defines efficiency as the ratio of the energy received by the detector to the total output energy of the LED light source. Non-uniformity is defined as the root-mean-square deviation from the average illuminance on the

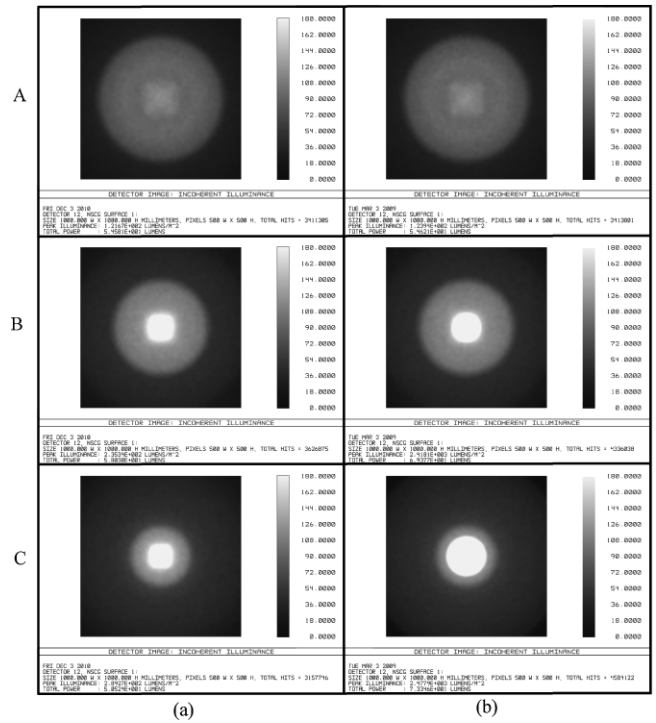


Fig. 5. Illuminance maps of the three configurations (a) with single inner reflector and (b) with inner and outer reflectors.

detector in the floodlight range excluding the central spotlight. The smaller the non-uniformity the better the uniformity for the illuminance distribution. This study compares the efficiencies and uniformities of the initial design with those from the following optimized designs.

4. Optimization

Optimizations were performed to improve the initial design in terms of floodlight uniformity and spotlight efficiency.

4.1 Merit function and design variable

To construct the merit function in this research, one circle (*I*) detector and six ring (*II* to *VII*) detectors were defined at the same position of the above-mentioned detector in Fig. 7. According to the illumination patterns of the above simulations, the maximum region of the spotlight corresponds to the regions *I* and *II*, and the following description calls this region the central zone. Because the floodlight region does not exceed the outer border of ring *VII*, the seven detectors can capture the entire illuminating pattern of the spotlight and floodlight. Different illuminating distributions could then be set as the merit function by manipulating the illuminance data from the detectors.

In this design, the inner and outer reflectors are the main components for controlling floodlighting and spotlighting, respectively. In other words, modifying the shape of one reflector will not change the collecting or distributing abilities of the other reflector. In addition, because the aperture sizes of the reflectors are fixed, reflector shape

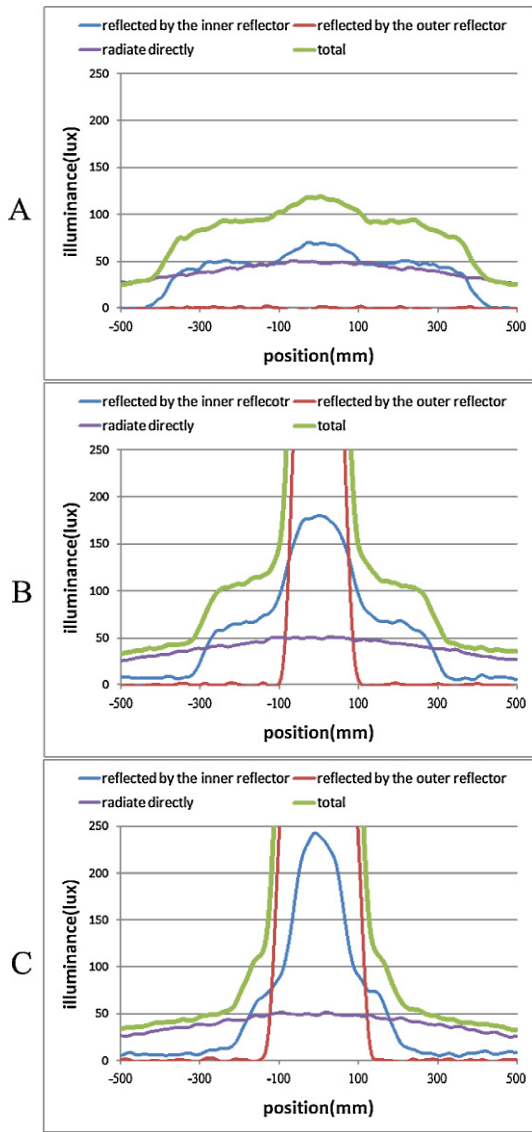


Fig. 6. (Color online) Cross-sectional illuminance values for the three configurations.

adjustments lead to relative changes in length. If the length of the inner reflector increases, the number of rays emitted to the outer reflector and the converging energy both decrease. For this reason, floodlight optimization was first performed to determine the shape of the inner reflector, and spotlight optimization was subsequently carried out to determine the shape of the outer reflector. This study adopted the orthogonal descent method as the optimization algorithm.

The inner reflector parameters c_{in} and k_{in} from the aspheric function served as the design variables for floodlight optimization, while the outer reflector parameters c_{out} and k_{out} from the aspheric function served as design variables for spotlight optimization.

4.2 Floodlight optimization

The major design goal of floodlight optimization is to increase the illumination uniformity in configuration A. In this case, most rays reflected by the outer reflector strike the

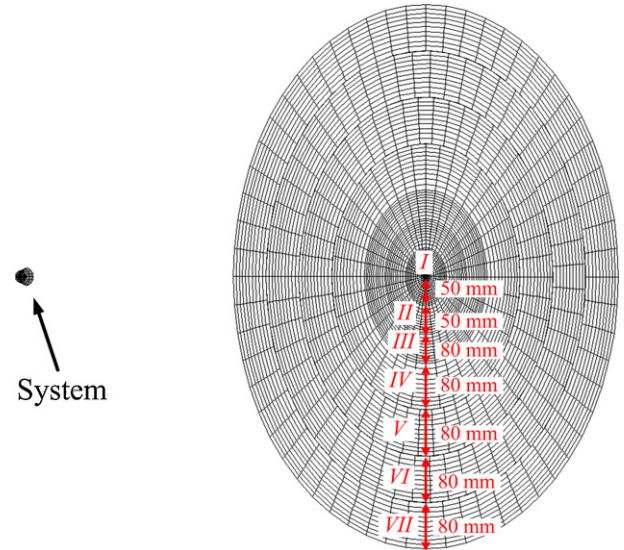


Fig. 7. (Color online) Ring detectors for optimization.

central zone and become high illumination. Hence, the floodlight configuration can achieve not only wide-range illumination, but long-distance illumination as well. For this reason, floodlight optimization considers the illuminating uniformity excluding that in the central zone. Besides, the total illuminance from all detectors should be increased as much as possible to avoid ray dispersion and maintain the original efficiency. Therefore, the merit function for floodlight optimization (U_{flo}) consists of four factors, including the ratios of the average illuminances from the detectors III to IV ($R_{III,IV}$), IV to V ($R_{IV,V}$), and V to VI ($R_{V,VI}$), and the illuminance summation from I to VII ($S_{I,VII}$). The design variables were c_{in} and k_{in} . A mirror property was applied to the inner reflector, while the outer reflector was assumed to be perfectly absorptive to eliminate its effect. Therefore, the floodlight optimization problem can be formulated as

$$\begin{aligned} & \text{Minimize } U_{flo}(c_{in}, k_{in}) \\ & \text{where } U_{flo}(c_{in}, k_{in}) = (R_{III,IV} - 1) + (R_{IV,V} - 1) \\ & \quad + (R_{V,VI} - 1) + \frac{1}{S_{I,VII}} \text{ in configuration A,} \end{aligned} \quad (2)$$

subject to

$$-1.5 < k_{in} < -1, \quad (3)$$

$$0.05 < c_{in} < 1. \quad (4)$$

4.3 Spotlight optimization

The goal of spotlight optimization is to configure the outer reflector to gather the maximum number of rays in the central zone in all configurations to achieve long-distance illumination. The merit function (U_{spo}) was then set as the inverse of the sum of the illuminances from the central zone, i.e., I and II ($S_{I,II}$), in configurations A, B, and C. The design variables were c_{out} and k_{out} , and the properties of the inner and outer reflectors were set to be perfectly absorptive and mirror-like, respectively. The spotlight optimization problem can be formulated as

Table 3. Comparisons of reflector parameters before and after optimizations.

	Inner reflector		Outer reflector	
	c^{-1} (mm)	k	c^{-1} (mm)	k
Before optimization	0.1	-1.3	2	-1.1
After optimization	0.104	-1.310	2.666	-1.057

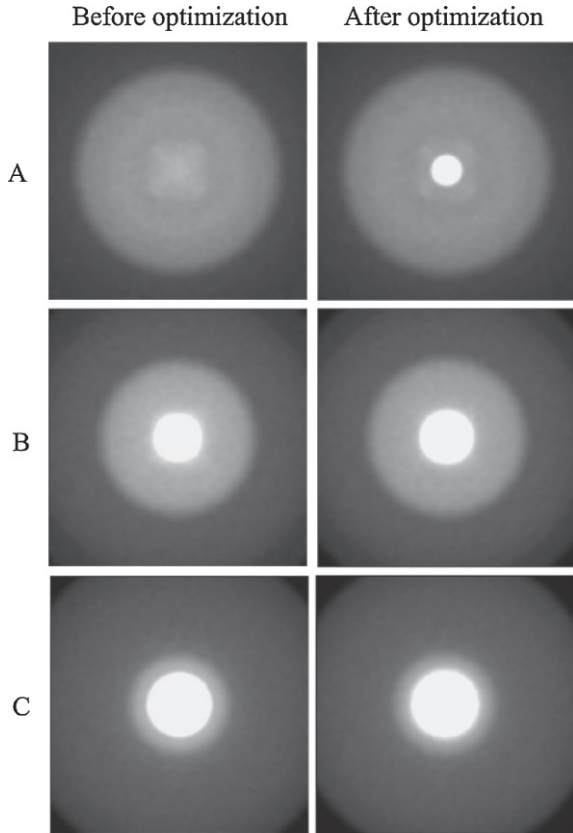


Fig. 8. Comparisons of illuminance maps for the three configurations before and after optimization.

$$\text{Minimize } U_{\text{spo}}(c_{\text{out}}, k_{\text{out}})$$

$$\text{where } U_{\text{spo}}(c_{\text{out}}, k_{\text{out}}) = \sum_{\text{configuration } A,B,C} \frac{1}{S_{L,II}}, \quad (5)$$

subject to

$$-1.5 < k_{\text{out}} < -1, \quad (6)$$

$$0.05 < c_{\text{out}} < 3. \quad (7)$$

4.4 Results

Table 3 lists the reflector parameters before and after floodlight and spotlight optimizations. Figure 8 compares the illuminance maps of the three configurations, and Fig. 9 displays the cross-sectional illuminance values. In configuration A, the non-uniformity decreased marginally from 13.96 to 10.90 lx, but the central illuminance increased

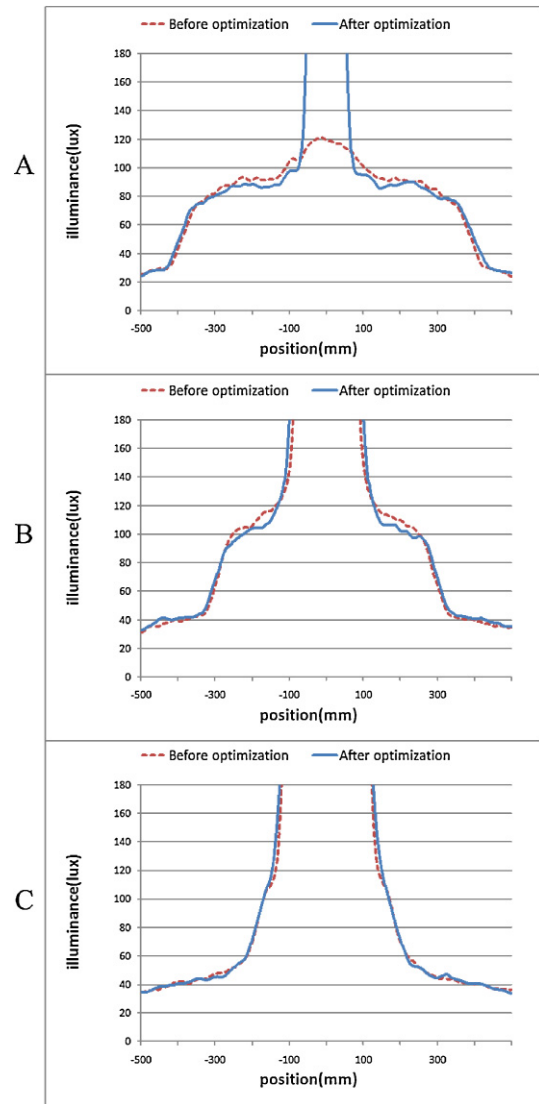


Fig. 9. (Color online) Comparisons of cross-sectional illuminance values for the three configurations before and after optimization.

Table 4. Comparisons of zoom process efficiencies before and after optimizations (unit: %).

	Configuration		
	A	B	C
Before optimization	68.3	86.7	91.7
After optimization	70.9	90.3	94.5

significantly and a focusing zone appeared. In configurations B and C, floodlight optimization is still inconspicuous, but Table 4 shows that the efficiencies increased in all configurations. Table 5 further indicates that optimization significantly enhances the maximum illuminances. Optimization clearly increased the spotlight, which is dominated by the outer reflector, but not the floodlight, which is governed by the inner reflector. This is because the initial design had already achieved an acceptable illuminance distribution, and

Table 5. Comparisons of maximum illuminance values for the three configurations before and after optimization (unit: lx).

	Configuration		
	A	B	C
Before optimization	123.9	2418.1	2477.9
After optimization	508.3	4053.0	4045.2

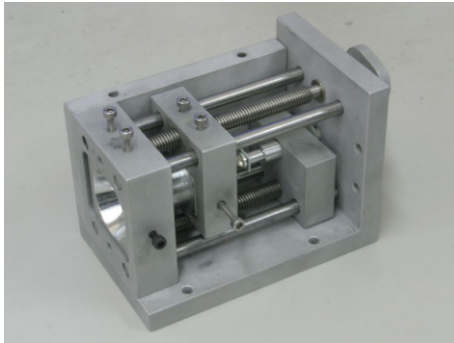


Fig. 10. (Color online) Apparatus for verification experiment.

Table 6. Corresponding positions for the simulated and experimental configurations.

For simulation	A					B
For experiment	<i>a</i>	<i>b</i>	<i>c</i>	<i>d</i>	<i>e</i>	
<i>X</i> (mm)	2	1.5	1	0.5	0	
<i>Y</i> (mm)	9	8	7	6	5	

the starting values of the design variables already approached the optimized values. Generally speaking, the optimization methods used in this research improved the initial design.

5. Verification Experiment

The light source, inner reflector, and outer reflector are the main components in the proposed design, and the zoom function is achieved by their relative movements. Therefore, at least two of the components should be displacement adjustable to achieve this purpose. Figure 10 shows the apparatus built for verification experiments in this study. The outer reflector was fixed, and the inner reflector and the light source were moveable by adjusting independent screws. Components were replaceable for different experiments. This study only tested configurations A to B because of the geometrical limit between the aperture of the reflector and the selected XR-E P4 LED light source. Table 6 shows the corresponding positions for the simulated and experimental configurations. Additional simulations on configurations *b* to *d* were performed for the following comparisons.

Figure 11 shows the simulated and experimental illuminance maps for configurations *a*, *c*, and *e*, revealing good consistency. Figure 12 shows that the cross-sectional values of illuminance have similar tendencies in all configurations, but the experimental values are lower than the simulated

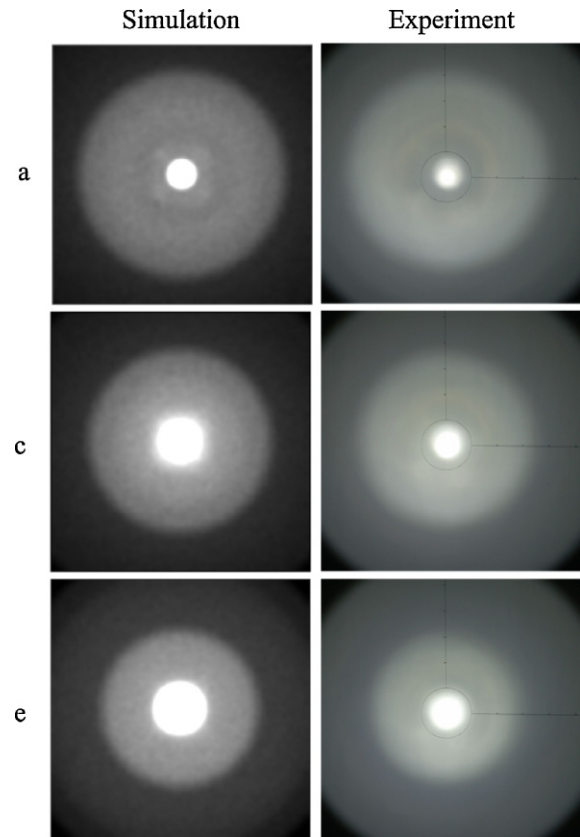


Fig. 11. (Color online) Comparisons between simulated and experimental illuminance maps for the three configurations.

results by about 10lx. Table 7 compares the maximum illumination values. The variation in this table indicates the illuminance percentage difference between experimental and simulated results. The lower experimental data might be the result of imperfect reflection by the reflectors. The variation values in Table 7 increase progressively from configuration *a* to *e*. This is because during the zoom process the area of the outer reflector that controlled the light increased, and the energy lost from the imperfect reflection also increased.

6. Conclusions

This study proposes and investigates a novel LED zoom illumination design. Two hyperbolic shape reflectors were adopted, and the relative displacements between the light source and the inner and the outer reflectors enabled the zoom function. The optical simulation software ZEMAX was adopted to simulate system performance, and optimizations were performed to adjust the reflector parameters for better uniformity of the floodlight and higher efficiency of the spotlight. An experimental apparatus was also built to verify the system, and experimental results demonstrate the practicability of the design. Based on these results, this study offers the following findings:

1. A zoom function was achieved with two hyperbolic reflectors and the relative displacement of the components. The inner reflector governs the floodlight, and the outer reflector dominates the spotlight.

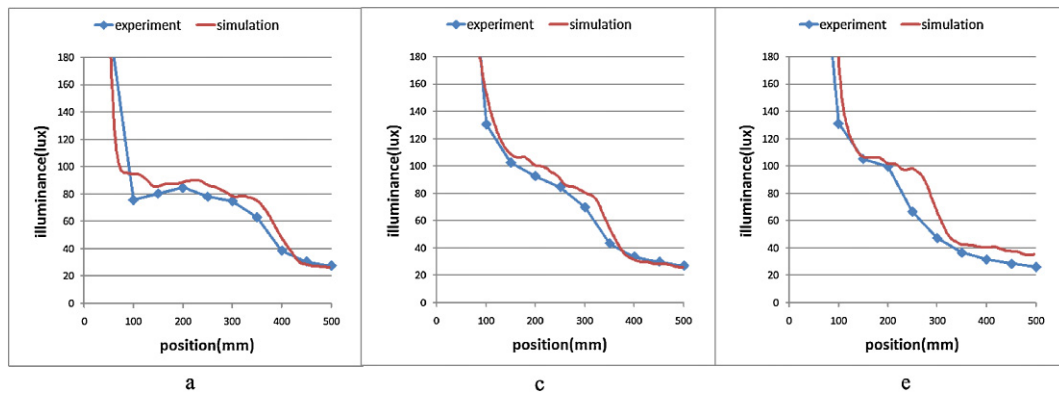


Fig. 12. (Color online) Comparisons of simulated and experimental cross-sectional illuminance values.

Table 7. Comparisons of simulated and experimental maximum illuminance values.

	a	b	c	d	e
Simulation (lx)	508	1195	2386	3476	4053
Experiment (lx)	300	659	1113	1184	1645
Variation (%)	41	45	53	66	59

- Optimizations were performed on both the inner and outer reflectors, improving the illuminance performance.
- Verification experiments were conducted for this new design. Although only parts of the configurations were tested, these experimental results are consistent with the simulated results, demonstrating the practicability of the design.

- Discrepancies between the predicted and experimental values may be due to the imperfect reflection of the reflector surfaces.

References

- D. A. Steigerwald, J. C. Bhat, D. Collins, R. M. Fletcher, M. O. Holcomb, and M. J. Ludowise: *IEEE J. Sel. Top. Quantum Electron.* **8** (2002) 310.
- W. B. Elmer: *IEEE Trans. Ind. Appl.* **19** (1983) 776.
- C. H. Tsuei, J. W. Pen, and W. S. Sun: *Opt. Express* **16** (2008) 18692.
- J. Hwang, K. H. Kim, J. H. Won, and E. S. Chung: *Proc. 5th Int. Conf. Nano/Micro Engineered and Molecular Systems*, 2010, p. 869.
- CREE, Inc. [<http://www.cree.com/>].
- D. Jenkins and M. Kaminski: *Proc. SPIE* **3130** (1997) 196.
- Focus Software, *ZEMAX Optical Design Program Users Guide*.